研　究　速　報

Evaluation of Electric Impedance Spectra for Single Bio-Cells in Microfluidic Devices using Combined FEMLAB/HSPICE Simulated Models

Vincent SENEZ*, Takatoki YAMAMOTO**, Benoit POUSSARD**,
Tatsuhiro FUKUBA**, Jean-Marc CAPRON*** and Teruo FUJII**

1. Introduction

Microfabrication techniques that have revolutionized the electronics industry, are now entering into the pharmaceutical, biotechnology and biotechnology device industries. The two leading applications of microfabrication in biology include "genes-on-a-chip" to monitor the expression level of genes in various organisms and "lab-on-a-chip" type devices to perform biochemistry in microchambers. However, biomedical application of microfabricated devices is not limited to non-living systems such as genes-on-a-chip or lab-on-a-chip.

Recent advances in the understanding of cellular behavior in microenvironments have allowed the design and fabrication of microdevices containing living organisms. Cell work has traditionally been done with equipment that is many orders of magnitude larger in size than a cell. As a consequence, it is difficult for a cell to maintain a microenvironment (i.e.: diffusion distance, stress, etc...) and it is assumed that its behavior in macroscale devices is different than *in vivo* conditions.

On the contrary, microdevices made from the proper materials (e.g.: gas-permeable polymers) allowing adequate oxygenation (without stirring or bubbling) and uniform nutrients diffusion are the perfect tools to conduct cell-based experiments at the microscale. The rich assortment of living microdevices that can be built using Bio-MEMS techniques have important applications in fundamental cell biological studies, tissue engineering, cell separation and culture devices, diagnostics, high-throughput drug screening tools, and cellular bio-detection.

Biological cells are spatially organized into membranes, organelles, and cytoskeleton. When culture is initiated, they connect to each other generating a higher structural organization (i.e.: tissue). Cellular physiological function is determined by myriad of biochemical reactions and biophysical processes coordinated in time and space by cellular control mechanisms. Living cells have many interesting properties: they offer miniature size, biological specificity, signal amplification, surface binding capability, self-replication, multivariate detection, and other benefits. Their engineering requires rapid characterization methods. While current optical and chemical detection techniques[1-3] can effectively analyze biological systems, a number of disadvantages restrict their versatility. As examples: most samples must be chemically altered prior to analysis, and photobleaching can place a time limit on optically probing fluorophore-tagged samples. Purely electronic techniques provide solutions to many such problems, as they can probe a sample and its chemical environment directly over a range of time scales, without requiring chemical modifications[4-5].

One example of electronic detection is electrical impedance spectroscopy (EIS)[6-8]: examining permittivity as a function of frequency. EIS is a non-invasive method for characterising cells suspensions or tissues. Because currents will pass either around or through cells depending on the frequency, EIS can be used to observe the structure and arrangement of cells.

Nowadays, the advances in the manufacture of microdevices and microelectrodes permit to place single cells or cultured cells in small cavities[9-13].

The objectives of this project is to demonstrate that viability of biocells (in terms of the integrity of their plasma membrane), size, shape and surface morphology of the cell plasma membrane can be discerned on the basis of microelectric impedance spectra (μ-EIS) data. The applications of this study include the ability to: 1) Separate cells for identification and enumeration, 2) Separate rare target cells from heterogeneous samples, avoiding cell loss, 3) Isolate viable, culturable cells with little or no biological damage, 4) Characterize the environment of cell cultures.

Hybrid microtechnologies (Silicon/Elastomer) are used to fabricate channels or cages containing single or cultured cells. Polydimethylsiloxane (PDMS) has been chosen to fabricate the microfluidic parts. A process has been developed allowing the integration of metal microelectrodes directly on PDMS.

*LIMMS/CNRS-IIS, The University of Tokyo
**UTRC/IIS, The University of Tokyo
***IEMN/CNRS (Villeneuve d'Ascq-France)

Computational modeling (FEMLAB & HSPICE) is used to optimise the morphology of the device and understand the effects of various biological parameters on the impedance of the system. First prototypes have been fabricated and are under test. We are currently designing the electronic instrumentation to record the EIS (30kHz–30MHz) of these single or cultured cells in order to ensure a high accuracy of the experimental data.

2. Modeling Strategy

μ-EIS accuracy depends on the design of both the sensor and the electronic interface. We are currently working on these two aspects. This paper summaries our work on the optimisation of the sensor. The use of four-electrode set-up (Fig. 1) increases the linearity, accuracy and sensitivity of the measurement[14].

The purpose of the study is to determine the size of the outer and inner electrodes and their location in the sensing area. Traditional approaches use Laplace equation in combination with the finite element (FE)[10]. Recently, this problem has been solved using Kirchhoff laws and transport lattice (TL) method[11].

In our approach, the advantages of these two methods are coupled. Indeed, the system being studied (i.e.: the microfluidic device) is divided into small finite elements (i.e.: triangles in 2D, tetrahedra in 3D) using the automatic mesh generator of FEMLAB (COMSOL). The initial mesh is refined around small geometrical features like the cell membrane (Fig. 2).

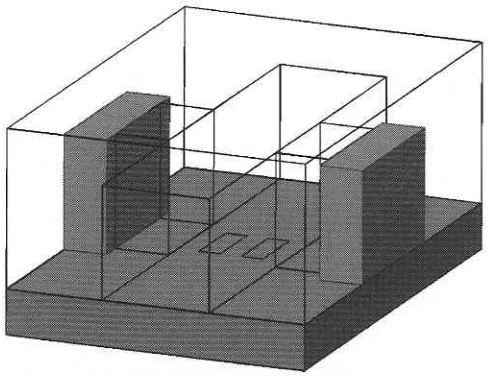

Fig 1　3 D schematic of the micro-EIS sensor.

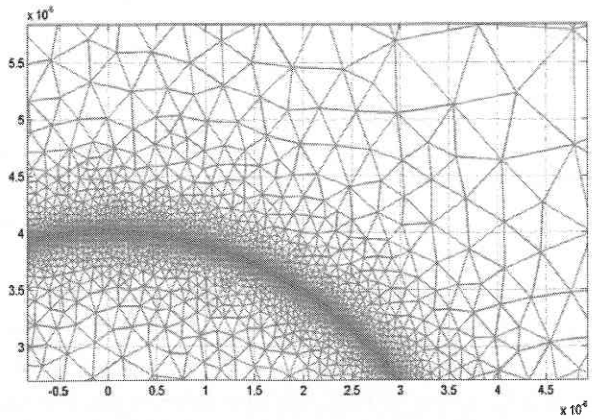

Fig 2　Details of the triangular FEM mesh obtained with FEMLAB. Automatic refinement of the cell membrane can be seen.

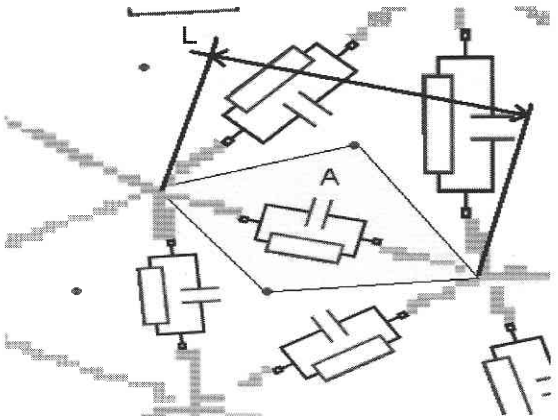

Fig 3　Details of the transport lattice. TL and FE nodes are located at the same position. Barycenters of triangles defined the surface represented by the local RC element.

Then, the data structure is exported to the MATLAB (MATHWORKS) environment where the TL is defined. In our implementation, the nodes of the TL corresponds to the nodes of the FE mesh (Fig. 3).

Finally, the TL is solved by Kirchhoffs laws, using HSPICE (SYNOPSIS) giving electrical currents and voltages through the lattice. 2D results are presented in this paper and we are currently working at the implementation of the 3D models. The 2D TL is composed of basic electrical elements (Fig. 3), consisting of a resistance (R_i) in parallel with a capacitance (C_i) where the subscript "i" defined the region of the system (i.e.: PDMS, electrodes, extra-cellular medium, membrane, cytoplasm).

3. Validation and Optimisation

First, we have compared the results (in terms of characteristic frequency or voltage) obtained by i) the FE method (FEMLAB), ii) the Weaver's approach[15] using HSPICE and iii) our own method with the corresponding analytical results. Plate capacitors with: i) one material, and ii) two different materials inserted as slab in series (Fig. 4a), or as a disk in a square (Fig. 4b) have been simulated.

We have studied the effect of the lattice density on the results. Table 1 gives the details of these validations.

Second, we have analysed the influence of several geometrical parameters on the variation of the impedance ($\Delta R/R = [Z_{\text{without Cell}} - Z_{\text{with Cell}}] / Z_{\text{without Cell}}$) due to one cell. Fig. 5 gives the 2D cross-section of the device used for the simulations. We have investigated: i) the height of the microchannel (Fig. 6a), ii) the widths of the

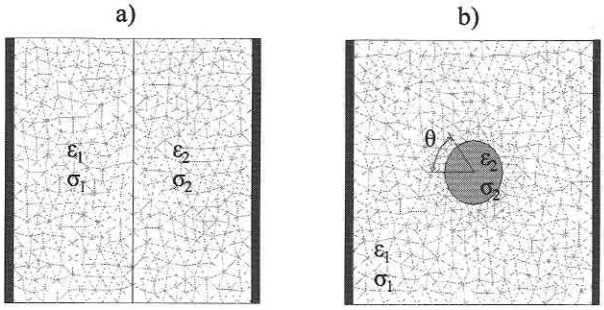

Fig 4 Test structures consisting in plate capacitors with different materials inserted as a) slab in series, or b) a disk in a square

Table 1 Simulation errors compared to analytical models and typical simulation times (800 triangles or 2500 RC elements).

Structure	Error (%)
Plate Capacitor (1 material)	1.5
Plate Capacitor (2 slabs)	2.7
Plate Capacitor (1 disk in a square)	5.5
Simulation Type	Time (s.)
HSPICE	12
FEMLAB	1560

outer and inner electrodes and iii)the distance between the outer electrodes (Fig. 6b).

In Fig. 6, one can see that the decrease of the micro-channel thickness and the increase of the distance between the outer electrodes improve the sensitivity at low frequency while they deteriorate this sensitivity at intermediate frequencies (Mhz). The simulation have also shown (not presented in this paper) that the width of the outer electrodes has no effect on the sensitivity at all frequencies; that the best sensivity is obtained when the inner electrodes are close to each others; and that the widths of the inner electrodes has to be small at low frequencies and large at intermediate frequencies. As a result of this work, we have defined an optimised sensor.

For a geometrical configuration giving the highest ΔR/R at low and intermediate frequencies, we have studied the effects of: i) the radius of the cell, ii) the conductivity of the extra-cellular medium and cytoplasm (Fig. 7a), iii) the thickness of the membrane (Fig. 7b).

One can observe in Fig. 7a that the increase of the cell membrane thickness has no effect on the sensitivity at low and intermediate frequencies. It only shifts the sensitivity curve to higher frequency since the cell is less transparent to the electrical current. In Fig. 7b, one can observe that the increase on the conductivity of the cytoplasm has no effect at low frequencies and increase the sensitivity at intermediate frequencies.

Our simulations show also (not presented in this paper) that the increase of the conductivity of the extra cellular medium increases the sensitivity at both low and intermediate frequencies. Finally, the increase of the radius of the cell increases the sensitivity more at low frequencies than at intermediate frequencies. For these simulations, we have used the following values as default parameters: $\varepsilon_{PDMS} = 2.65\varepsilon_0$; $\sigma_{PDMS} = 0.5\text{x}10^{-17}\text{Sm}^{-1}$; $\varepsilon_{Glass} = 4.2\varepsilon_0$; $\sigma_{Glass} = 10^{-14}\text{Sm}^{-1}$; $\varepsilon_{Electrode} = 0\text{Fm}^{-1}$; $\sigma_{Electrode} = 4.5\text{x}10^{5}\text{Sm}^{-1}$; $\varepsilon_{Electrolyte}$

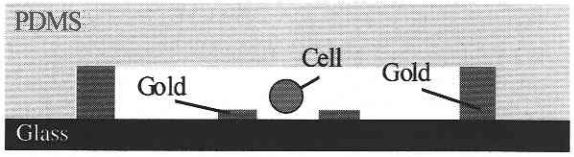

Fig 5 2 D cross-section of the simulated device. The outer electrodes are either planar or 3 D.

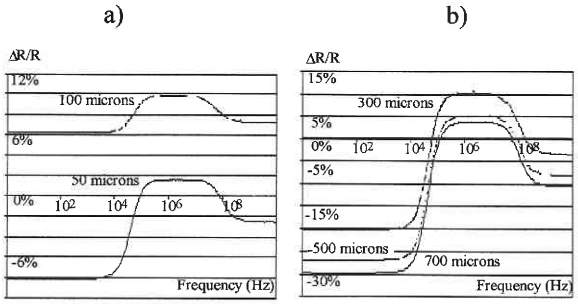

Fig 6 Calculated influence of: a) the height of the channel, b) the distance between the outer electrodes on the impedance spectrum from 1 Hz to 10 GHz.

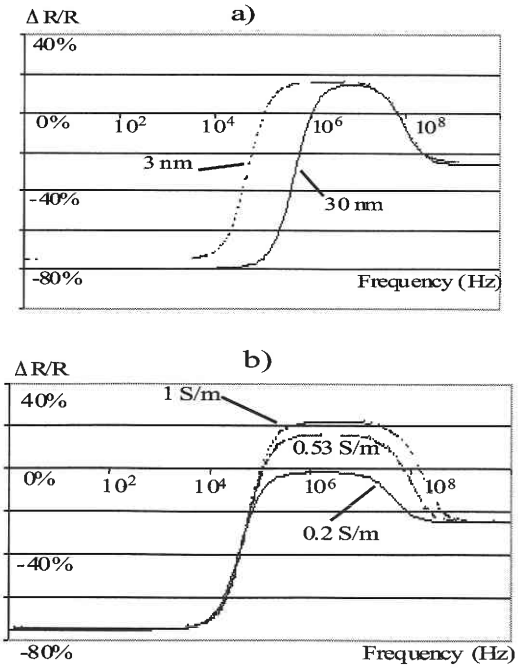

Fig 7 Calculated influence of: a) the thickness of the cell membrane, b) the conductivity of the cytoplasm on the impedance spectrum from 1 Hz to 10 GHz.

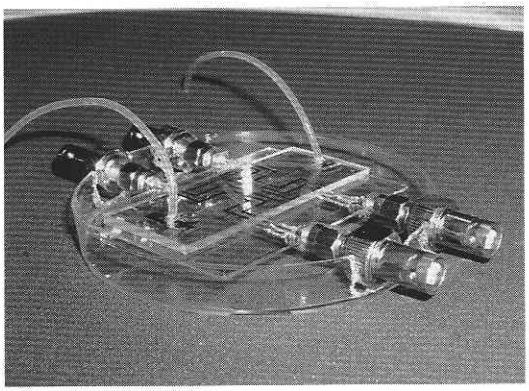

Fig 8 First prototype of the μ-EIS sensor using planar gold outer electrodes.

$= 80\varepsilon_0$; $\sigma_{Electrolyte} = 0.12 Sm^{-1}$; $\varepsilon_{Membrane} = 9.04\varepsilon_0$; $\sigma_{Membrane} = 10^{-6} Sm^{-1}$; $\varepsilon_{Cytoplasme} = 50\varepsilon_0$; $\sigma_{Cytoplasme} = 0.53 Sm^{-1}$).

First prototypes are under fabrication (Fig. 8) and our simulated results will be compared in a near future to experimental data.

4. Conclusion

We have implemented a tool for fast simulation of the effect of the electric field on cells. It uses 2D transport lattice method to calculate the distribution of the electrical potential and current in a μ-EIS device containing a living organism. The geometrical features of this μ-sensor have been optimised and the device is now under fabrication. We are currently improving this method to allow 3D modelling. In parallel, we have designed an electronic interface to accurately record the EI spectrum that is now under implementation.

This work will be presented at the 2004 Nanotechnology Conference and Trade Show, March 7–11, 2004, Boston, Massachusetts, U.S.A..

Acknowledgments

We thank Dr E. Leclerc and Dr S. Ostrovidov (LIMMS/CNRS-IIS) for fruitfull discussion about cells culture in micro-devices. We would like also to acknowledge Prof. Y. Mita for assistance with the computers facilities of VDEC (VLSI Design and Education Center) at the University of Tokyo.

This project is under study in the framework of LIMMS, the Laboratory for Integrated Micro Mechatronic Systems, located in Tokyo, a joint laboratory between the Communication and Information Science and Technology Department of CNRS (CNRS-STIC, France) and the Institute of Industrial Science (IIS) in the University of Tokyo. It is supported by the CNRS, the MEXT (Japanese Ministry of Education, Culture, Sports, Science and Technology), and the JSPS (Japanese Society for the Promotion of Science).

Part of the photomask fabrication was also performed using VDEC facilities.

（Manuscript received, November 26, 2003）

References

1) S. Nie and R. N. Zare, Annu. Rev. Biophys. Biomol. Struct., **26**, 567, (1997).
2) S. Weiss, Science, **283**, 1676, (1999).
3) G. MacBeath and S. L. Schreiber, Science, **289**, 1760, (2000).
4) J. Viovy, Rev. Mod. Phys., **72**, 813, (2000).
5) L. L. Sohn, O. A. Saleh, G. R. Facer, A. J. Beavis, R. S. Allan, and D. A. Notterman, Proc. Natl. Acad. Sci. U.S.A., **97**, 10687, (2000).
6) K. Asami, E. Gheorghiu, and T. Yonezawa, Biophys. J., **76**, 3345, (1999).
7) C. Prodan and E. Prodan, J. Phys. D, **32**, 335, (1999).
8) G. Smith, A. P. Duffy, J. Shen, and C. J. Olliff, J. Pharm. Sci., **84**, 1029, (1995).
9) J. Gimsa, T. Muller, T. Schnelle and G. Fuhr, Biophys. Journal, **71**, 495, (1996).
10) S. Gawad, L. Schild and Ph. Renaud, Lab on a Chip, **1**, 76, (2001).
11) H.E. Ayliffe, S.D. Brown, and R.D. Rabbitt, Proc. 2nd Joint EMBS/BMES Conf., Houston, 1692, (2002).
12) H.E. Ayliffe, R.D. Rabbitt, P.A. Tresco, A. B. Frazier, Proc. Transducers, Chicago, 1307, (1997).
13) R. Pethig, J.P.H. Burt, A. Parton, N. Rizvi, M.S. Talary, and J.A. Tame, J. Micromech. Microeng., **8**, 57, (1998).
14) F. Laugere *et al.*, Sens. Actuators, **A92**, 109, (2001).
15) T. Gowrishankar and C. Weaver, PNAS, **100**, 3203, (2003).